

See discussions, stats, and author profiles for this publication at: <https://www.researchgate.net/publication/234017480>

Estimating the Water Retention Shape Parameter from Sand and Clay Content

ARTICLE in SOIL SCIENCE SOCIETY OF AMERICA JOURNAL · JULY 2007

Impact Factor: 1.72 · DOI: 10.2136/sssaj2006.0298N

CITATIONS

34

READS

81

2 AUTHORS:



[Budiman Minasny](#)

University of Sydney

323 PUBLICATIONS **5,576** CITATIONS

[SEE PROFILE](#)



[Alex B Mcbratney](#)

University of Sydney

493 PUBLICATIONS **13,766** CITATIONS

[SEE PROFILE](#)

Estimating the Water Retention Shape Parameter from Sand and Clay Content

Budiman Minasny*

Alex B. McBratney

Faculty of Agriculture
Food & Natural Resources, A05
The Univ. of Sydney
Sydney, NSW 2006
Australia

This study developed an alternative way of estimating the van Genuchten water retention shape parameter n from a soil's sand and clay content. This estimation can be used to complement an infiltration experiment called the Beerkan method, which has been proposed for estimating the van Genuchten water retention function and Brooks–Corey hydraulic conductivity characteristic. To estimate the water retention shape parameter, the Beerkan method requires a distribution function fitted to particle-size distribution data (more than five fractions) and a measurement of bulk density. Using three published databases, we were able to derive a neural network model that predicts the shape parameter and its uncertainty from sand and clay content. Its accuracy ranges from 0.2 to 0.4. This method is comparable to prediction using parameterized particle-size distribution data. The response surface of n as a function of sand and clay content shows an increasing value of n with increasing sand content in a nonlinear way. We also show that using simpler methods for predicting shape parameter n does not influence the accuracy of the Beerkan method in estimating the soil hydraulic properties.

Abbreviations: GRIZZLY, Grenoble soil catalog, PSD, particle size distribution; UNSODA, unsaturated soil hydraulic database.

BRAUD ET AL. (2005) and Lassabatère et al. (2006) proposed an infiltration method, called the Beerkan method, for estimating soil hydraulic properties. This involves an infiltration experiment in the field using a ring with pressure head $h = 0$ at the soil surface. It provides an estimate of not only saturated hydraulic conductivity, but also water retention and hydraulic conductivity characteristics. One of the requirements, however, is to estimate the shape parameter of the water retention curve from particle-size distribution data and the soil's porosity. At least five measurements of particle size fractions are needed to characterize particle size distribution (PSD) properly. In many conventional laboratory analyses, particle size is only provided in three or four fractions. Furthermore, in many instances, particle

size analysis is not available and field texture (hand texture) may be the only data that was collected.

We examined whether the shape parameter can be predicted solely from the sand and clay fraction. This will make the Beerkan method more practical in the field with a much lower cost. While there are many pedotransfer functions predicting water retention parameters (Schaap et al., 1998), they take a different form from the one used by Lassabatère et al. (2006). The objective of this study was to derive an empirical pedotransfer function for predicting the shape parameter n from sand and clay content that can be used in the Beerkan method. We compared its accuracy with prediction using the standard method using the particle size distribution function and evaluated its influence on the Beerkan hydraulic parameters estimation method. We developed a surface of the shape parameter, and determined the influence of particle size on the water retention function.

THEORY

The analysis of the Beerkan infiltration experiment is based on an analytical solution of three-dimensional infiltration with defined hydraulic characteristic functions (Braud et al., 2005). The water-retention function is modeled following the van Genuchten (1980) equation:

$$\frac{\theta(h)}{\theta_s} = \left[1 + \left(\frac{h}{h_g} \right)^n \right]^{-m}, \text{ with } m = 1 - \frac{2}{n} \quad [1]$$

where θ is water content [$L^3 L^{-3}$], θ_s is saturated water content [$L^3 L^{-3}$], h_g is a scale parameter [L], and n is a dimensionless shape factor with condition $n > 2$. This function has a residual water content θ_r fixed at 0. Hydraulic conductivity is modeled based on the Brooks and Corey (1964) equation:

$$\frac{K(\theta)}{K_s} = \left(\frac{\theta}{\theta_s} \right)^\eta \quad [2]$$

where K is hydraulic conductivity [$L T^{-1}$], K_s is saturated hydraulic conductivity [$L T^{-1}$], and η is a conductivity shape factor that can be related to n by

$$\eta = \frac{2}{\lambda} + 2 + p, \text{ with } \lambda = mn \quad [3]$$

where p is a tortuosity parameter that depends on soil type. A value of 1 is used here following Burdine's condition (Burdine, 1953; Braud et al., 2005).

The Beerkan method measures cumulative infiltration with time; in addition, it requires measurement of bulk density, initial and saturated water content θ_s , and the PSD of the soil. Saturated hydraulic conductivity K_s is estimated from the infiltration data. The soil-water retention shape parameter n is estimated from the soil's particle size distribution function and porosity. Parameter h_g is estimated from sorptivity, K_s , and the shape parameter n (Lassabatère et al., 2006).

Estimation of n is based on the soil's particle size distribution function, which is modeled as

$$F(D) = \left[1 + \left(\frac{D_g}{D} \right)^N \right]^{-M}, \text{ with } M = 1 - \frac{2}{N} \quad [4]$$

where $F(D)$ is the cumulative PSD, D is the effective diameter of soil particles [L], D_g is a scale parameter [L], and N and M are dimensionless shape factors. The assumption is that the shape of the particle-size function N can be related to the water-retention curve n via their shape index (Haverkamp et al., 2005). The shape index, which is the

Soil Sci. Soc. Am. J. 71:1105–1110

doi:10.2136/sssaj2006.0298N

Received 23 Aug. 2006.

*Corresponding author (b.minasny@usyd.edu.au)

© Soil Science Society of America

677 S. Segoe Rd. Madison WI 53711 USA

All rights reserved. No part of this periodical may be reproduced or transmitted in any form or by any means, electronic or mechanical, including photocopying, recording, or any information storage and retrieval system, without permission in writing from the publisher. Permission for printing and for reprinting the material contained herein has been obtained by the publisher

Table 1. Mean and standard deviation of soil physical properties of the three databases used in this study.

Property	Australia	GRIZZLY	UNSODA
Clay content, % (w/w)	28.6 ± 16.5	20.6 ± 19.4	16.8 ± 14.0
Sand content, % (w/w)	40.0 ± 21.4	44.7 ± 31.1	54.2 ± 31.1
Bulk density, Mg m ⁻³	1.43 ± 0.22	1.46 ± 0.19	1.46 ± 0.23
<i>n</i>	2.29 ± 0.48	2.30 ± 0.43	2.71 ± 1.75
ln(<i>h_g</i>), ln(mm)	5.51 ± 1.83	5.89 ± 1.40	5.55 ± 1.76

integral of the slope of the log-transformed water retention curve, is defined as

$$p_m = \frac{mm}{1+m} \quad [5]$$

while for the particle-size distribution:

$$p_M = \frac{MN}{1+N} \quad [6]$$

They are related by

$$p_m = \iota p_M \quad [7]$$

where ι is a scaling parameter to translate particle size to pore size distribution, which depends on soil porosity (Braud et al., 2005):

$$\iota = \frac{1-s}{2-s-(1/2s)} \quad [8]$$

and s is a fractal pore measure that can be found from the solution of (Fuentes et al., 1998):

$$\varepsilon^{2s} + (1-\varepsilon)^s = 1, \quad 0.5 \leq s \leq 1 \quad [9]$$

where ε is soil porosity, which is estimated from bulk density. We simplify Eq. [8–9] by an fitting a cubic polynomial to the empirical observations between ι and ε :

$$\iota = 0.7467 - 0.6266\varepsilon + 0.5456\varepsilon^2 - 0.3813\varepsilon^3 \quad [10]$$

which has an average absolute error of 6×10^{-5} in the range $0.3 \leq \varepsilon \leq 0.7$.

To fit Eq. [4] to the particle size data adequately, we need at least five measurements. In this study, we derived the shape parameter from the sand and clay fractions. While there are many pedotransfer functions predicting van Genuchten parameters from sand, silt, and clay content (Schaap et al., 1998; Minasny and McBratney, 2002b) they are derived from the original form of van Genuchten (1980) i.e., $\theta_r \geq 0$ and $m =$

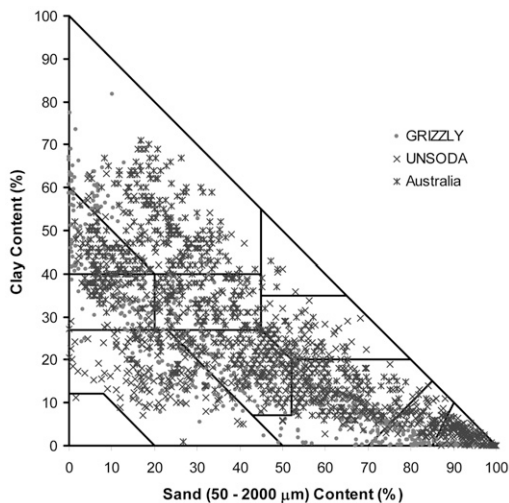


Fig. 1. Distribution of soil texture from the three soil hydraulic databases used in this study.

$1 - (1/n)$. The shape factor n will be different when the van Genuchten function is fitted to the data with and without θ_r (Leij et al., 2005).

MATERIALS AND METHODS

Soil Hydraulic Properties Data Set

We used three soil databases with hydraulic properties and particle size distribution: the unsaturated soil hydraulic database UNSODA, the Grenoble soil catalog GRIZZLY, and the Australian soil database. We selected 630 samples that contained particle-size data and laboratory-determined water retention curves from UNSODA (Leij et al., 1996). Water retention data were fitted to Eq. [1] using nonlinear least squares. Particle size distribution data that had more than four fractions (377 samples) were fitted to Eq. [4]. Sand (particles 50–2000 μm) and clay (<2 μm) content were derived from the particle-size data; when measurements using the USDA sand and clay fractions were not given, they were predicted using fitted Eq. [4]. The GRIZZLY database (Haverkamp et al., 1997; Haverkamp, personal communication, 2003) contains 660 samples. The database contains parameters of water retention and PSD according to Eq. [1] and [4]. Details on UNSODA and GRIZZLY databases can be found in Haverkamp et al. (2005).

The Australian soil hydraulic properties database (Minasny and McBratney, 2002b) has 972 samples and contains four fractions in the PSD measured according to the International system (<2, 2–20, 20–200, and 200–2000 μm). The sand fraction of the International system is converted to the USDA system using the function provided by Minasny and McBratney (2001). Water retention data were fitted to Eq. [1] using nonlinear least squares.

All three databases were combined, producing a data set of 2262 samples. The statistics of the physical properties of the three databases is given in Table 1. Figure 1 shows the distribution of the sand and clay content, which shows that they cover most of the textural triangle except silt. The sand texture is mainly populated by the UNSODA and GRIZZLY databases, while the clay texture comes mainly from the Australian database.

Predicting the Shape Parameter n

A first inspection shows that values of n increase in a steady manner with increasing sand content until about 70%, at which point the values increase rapidly (Fig. 2). A small value of n refers to a water retention curve with a gentle slope, implying a wide range of pore size distribution. A large value of n refers to sandy soils where the water retention curve has a prominent “leg” and a narrow range of pore sizes.

We used artificial neural networks to derive the relationship between clay and sand content with n . A neural network is a mathematical structure

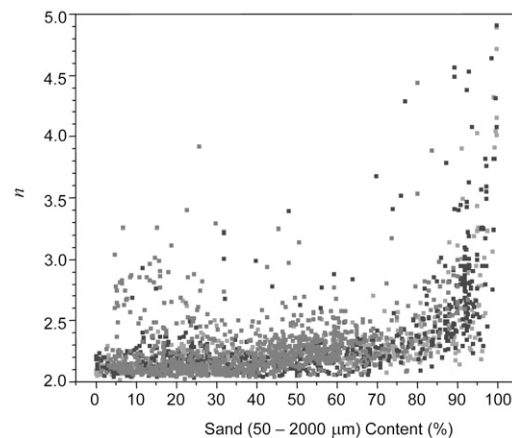


Fig. 2. The relationship between sand content and shape parameter n .

that consists of an interconnected assembly of simple processing elements. It has been used widely in soil science and hydrology to derive pedotransfer functions (Schaap et al., 1998; Minasny and McBratney, 2002b), to model complex relationships between inputs and outputs (Persson et al., 2002; Ancil et al., 2004), and generally to find patterns in data. An advantage of using a neural network, compared with conventional statistical methods such as multiple linear regression, is that no structure or relationships need to be assumed beforehand; instead, the network is adjusted or “trained” to find the relationship (Hastie et al., 2001).

We used the feed forward neural network model with three hidden nodes (Hastie et al., 2001; Schaap et al., 1998). Parameter n was transformed to $\ln(mn)$ to make it normally distributed and its value always >2 . To identify a suitable model, the combined data set was split into “training” (1508 samples) and “test” (754 samples) sets. When an appropriate model, in terms of providing accurate prediction on the test set, was identified, the neural network calibration was performed on all data. The criteria for goodness of fit are the mean and standard deviation of the residuals:

$$\text{residual} = \text{predicted} - \text{observed} \quad [11]$$

A good prediction will have a mean residual close to zero, while positive values indicate overestimation and negative values indicate underestimation. The standard deviation of the residuals measures the accuracy of prediction, representing the expected magnitude of error.

We used the bootstrap technique on neural networks (Efron and Tibshirani, 1993) to obtain the mean and standard deviation of prediction. The bootstrap technique assumes that the training data set is a representation of the population, and multiple realizations of the population can be simulated from a single data set. This is done by repeated “sampling with replacement” of the original data set of size d to obtain B bootstrap data sets, each with the size d . We used a $B = 50$ bootstrap, and $d = 2262$ for our data set.

Each bootstrap data set contains different data configurations and the neural net is trained on each of the bootstrap data, resulting in B neural networks. The bootstrap technique also allows for cross-validation of the model; for each bootstrap with “sampling with replacement,” approximately 63% of the original data will be used. About 37% of the original data is not used in training, so-called out-of-bag data (Breiman, 1996). The left-out data allows accuracy assessment of the prediction.

Influence of Predicted n on the Beerkan Estimation of Hydraulic Parameters

We investigated the effect of using predicted n using pedotransfer functions on the Beerkan estimation of hydraulic parameters. In the GRIZZLY database, there are 46 samples that contain measurement of $K(\theta)$ fitted to the Brooks–Corey equation (Eq. [2]) in addition to the water retention curve. For each soil sample, we used the observed or reported hydraulic parameters (θ_s , h_g , n , K_s , and η); we assumed an infiltration experiment was performed on the soil for 1 h with initial water content at a pressure head of -50 m and a ring radius of 100 mm. A theoretical infiltration curve was generated under this condition based on the equations proposed by Lassabatère et al. (2006):

$$I(t) = S\sqrt{t} + (AS^2 + BK_s)t \quad [12]$$

where S is sorptivity, and

$$A = \frac{\gamma}{r_d(\theta_0 - \theta_s)} \quad [12a]$$

$$B = \frac{2-\beta}{3} \left[1 - \left(\frac{\theta_0}{\theta_s} \right)^\eta \right] + \left(\frac{\theta_0}{\theta_s} \right)^\eta \quad [12b]$$

r_d is the radius of the ring [L], θ_0 is the initial water content [L^{-3}], $\gamma = 0.75$, and $\beta = 0.6$ (Haverkamp et al., 1994). Sorptivity is calculated from

$$S^2(\theta_0, \theta_s) = -c_p \theta_s K_s h_g \left[1 - \frac{\theta_0}{\theta_s} \right] \left[1 - \left(\frac{\theta_0}{\theta_s} \right)^\eta \right] \quad [13]$$

with

$$c_p = \Gamma \left(1 + \frac{1}{n} \right) \left[\frac{\Gamma \left(mn - \frac{1}{n} \right)}{\Gamma(mn)} + \frac{\Gamma \left(mn + m - \frac{1}{n} \right)}{\Gamma(mn + m)} \right] \quad [13a]$$

where Γ stands for the Gamma function.

This produced a cumulative infiltration curve $I(t)$ with time t from 0 to 1 h with a time step of 0.1 h. We then predicted n using the following methods:

- Method 1, the physical-based method of Lassabatère et al. (2006) which uses porosity and the parameters of the PSD (Eq. [5–9]).
- Method 2, our proposed method using sand and clay content (Eq. [18]).
- Method 3, our method given only the texture class.

Using the theoretical infiltration data $I(t)$, we fitted a Philip's two-term-type infiltration equation with linear least-squares method (Minasny and McBratney, 2000):

$$I(t) = C_1 \sqrt{t} + C_2 t \quad [14]$$

where C_1 is an empirical parameter equivalent to sorptivity [$L T^{-0.5}$] and C_2 is equivalent to the steady-state infiltration rate [$L T^{-1}$].

Using parameters C_1 , C_2 , and information on θ_0 , θ_s , and the predicted n , we calculated the other hydraulic parameters according to the procedures given in Lassabatère et al. (2006):

$$S = C_1 \quad [15]$$

$$h_g = - \frac{S^2}{K_s c_p (\theta_s - \theta_0) \left[1 - (\theta_0/\theta_s)^\eta \right]} \quad [16]$$

$$K_s = \frac{C_2 - AC_1^2}{B} \quad [17]$$

and η from Eq. [3].

This exercise assumes that the infiltration curve, θ_0 , θ_s can be measured accurately and the error only comes from the prediction of n .

RESULTS AND DISCUSSION

Predicting Shape Parameter n

First we tried two combinations of predictors to predict parameter n using neural networks: clay and sand content, and clay and sand content with bulk density. Results (Table 2) on the test set show that the inclusion of bulk density did not improve the prediction of n . The standard deviation of the residuals using only clay and sand is 0.435, while including bulk density gives 0.474. Thus we used only sand and clay content to predict n . We then generated neural networks with 50 bootstraps on all data; the average standard deviation of residuals for the out-of-bag data is 0.41. Thus, we are able to give an accuracy of our estimates of n as ± 0.4 . The average neural network prediction function can be written as

$$n = 2.18 + 0.11 [48.087 - 44.954S(x_1) - 1.023S(x_2) - 3.896S(x_3)] \quad [18]$$

where

Table 2. Means and standard deviations of residuals for prediction of shape parameter n with predictors sand and clay content, and sand and clay content and bulk density on the training and test sets.

Set	No. of samples	Predictor: sand, clay		Predictor: sand, clay, bulk density	
		Mean	SD	Mean	SD
Training set	1508	0.057	0.376	0.053	0.340
Test set	754	0.077	0.435	0.077	0.474

$$\begin{aligned} x_1 &= 24.547 - 0.238 \text{ sand} - 0.082 \text{ clay} \\ x_2 &= -3.569 + 0.081 \text{ sand} \\ x_3 &= 0.694 - 0.024 \text{ sand} + 0.048 \text{ clay} \end{aligned}$$

[18a]

sand and clay refer to sand and clay content (% w/w), and

$$S(x) = \frac{1}{1 + \exp(-x)}$$

[18b]

We compared our prediction with the physical-based method, which requires detailed particle-size data and porosity (Eq. [4–9]). Table 3 shows the comparison of the residuals of the prediction on the UNSODA and GRIZZLY databases. Figure 3 shows the fit of both methods of prediction. For the UNSODA database, neural networks give comparable prediction with the physical model, while for the GRIZZLY database the

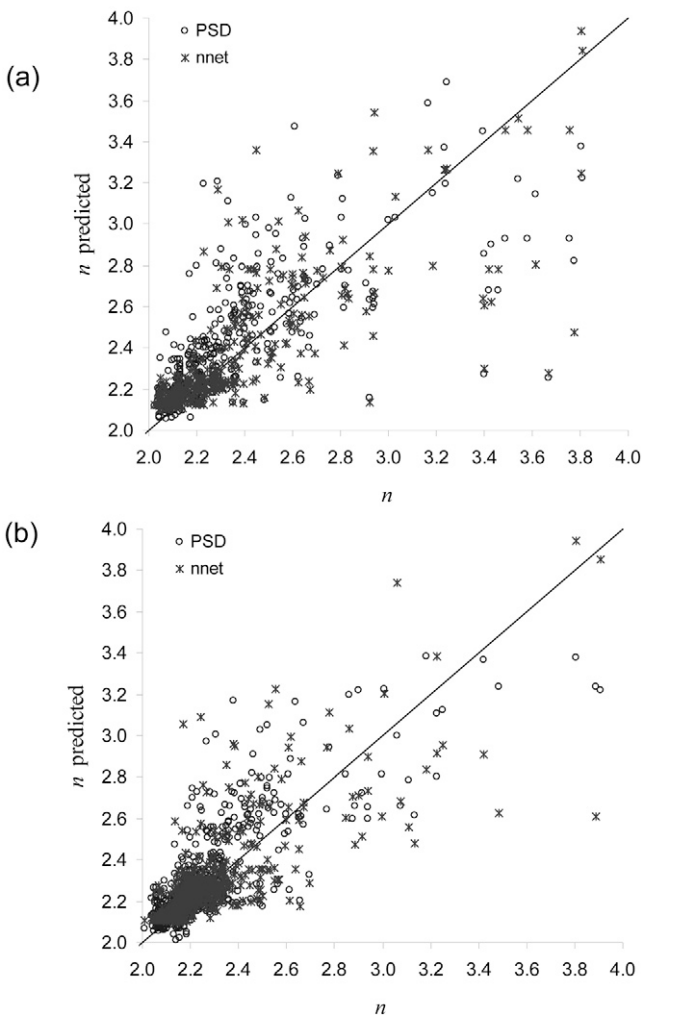


Fig. 3. Measured and predicted shape parameter n using a neural network (nnet, sand and clay content) and a physical model (PSD, particle-size distribution function and porosity) for (a) the UNSODA and (b) the GRIZZLY databases.

Table 3. Means and standard deviations of residuals for prediction of shape parameter n using a physical model (with particle-size distribution [PSD] function and soil porosity ϵ) and neural network (sand and clay content) for two databases.

Database	No. of samples	Physical model (PSD, ϵ)		Neural net (sand, clay)	
		Mean	SD	Mean	SD
UNSODA	377	0.023	0.736	0.087	0.713
GRIZZLY	660	−0.025	0.197	−0.001	0.233

physical model performs slightly better. In summary, the prediction of shape parameter n using sand and clay content is comparable with using detailed particle-size data and porosity. Thus our method can be used as an alternative when detailed particle size analysis is not available.

The surface of n as a function of sand and clay content is presented in Fig. 4a. As shown in the graph, the highest n is for the sand texture, and the value of n decreases with increasing clay content in a nonlinear pattern. The uncertainty (standard deviation) of the model is given in Fig. 4b, where the region of least uncertainty (standard deviation <0.01) is in the middle of the triangle (clay 10–70%) where most of the data lies (see Fig. 1). For

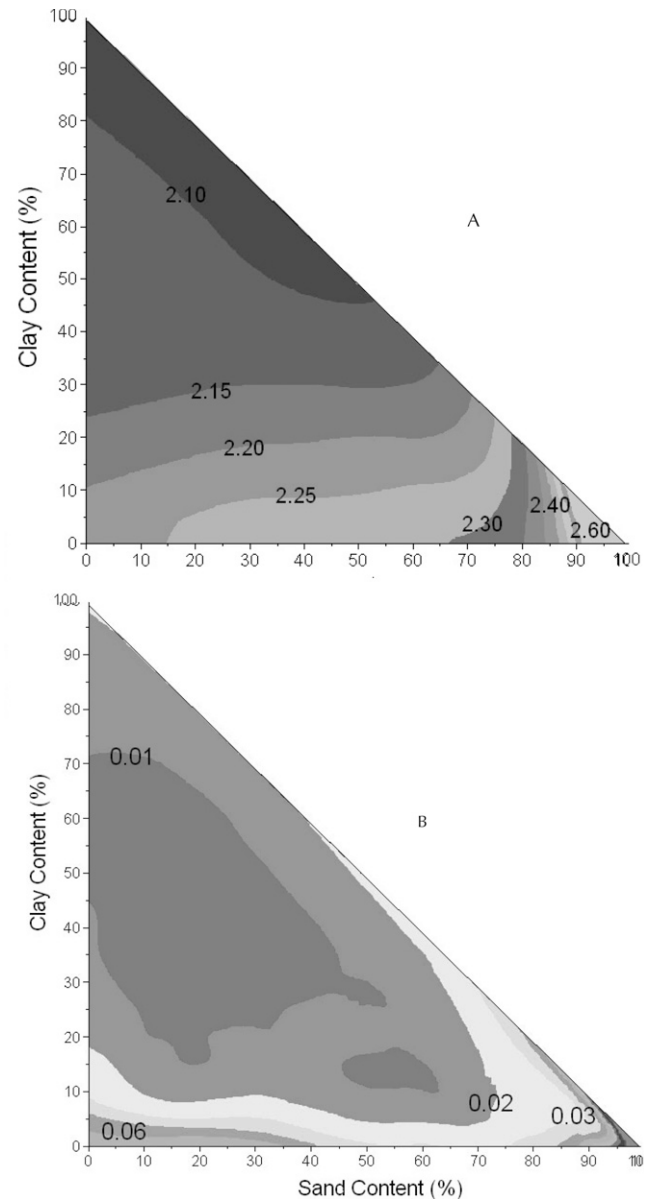


Fig. 4. Response surface of (a) predicted shape parameter n and (b) uncertainty in prediction as a function of sand and clay content.

the Brooks–Corey hydraulic conductivity shape parameter η (Fig. 5a), the highest value is found for clay, and values decrease with increasing sand content. The value of the shape index p_m (Fig. 5b) conforms to the observation shown by Haverkamp et al. (2005, Fig. 9).

From the response surface (Fig. 3, 4, and 5), we calculated the average of estimated parameters n , η , and p_m for each texture class (Table 4). The uncertainty becomes larger—the error propagation can be seen in the estimation of η ; for example for the silt texture where there are little calibration data, the uncertainty becomes large.

The Effect of Predicted n on the Beerkan Estimation of Hydraulic Parameters

Table 5 shows the influence of predicted n on the estimation of K_s , h_g , and η using the Beerkan infiltration experiment. The results showed that all three methods give similar prediction of n ; only the physical method (Method 1) tends to overestimate it. Values of K_s do not appear to be influenced by the different methods of estimation of n . From Eq. [17] we can see that values of K_s are mostly governed by parameter C_2 (or the steady-state infiltration rate). Estimation of h_g has a large error with standard deviation of residuals around 550 mm. This error translates into a larger error when estimating the water retention curve. Table 5 also shows prediction of water retention and hydraulic conductivity at 10, 100, 1000, and 5000 mm of suction. Water retention at low suction (near saturation) can be predicted very well. The predictions have larger errors when the suction is high (drier). Meanwhile the hydraulic conductivity function is predicted very well; this is because parameter η is mainly influenced by prediction of n .

Figure 6 shows prediction of water retention and hydraulic conductivity curves for three soil types: sand, sandy loam, and clay. Water retention can be predicted reasonably well for sand, while for sandy loam and clay the prediction deviates with increasing suction. Meanwhile, all three methods predicted hydraulic conductivity very well.

This study demonstrated that using alternative (simpler) methods for predicting shape parameter n does not influence the accuracy of the Beerkan method in predicting soil hydraulic properties. Hydraulic conductivity curves can be predicted reasonably well (assuming that they conform to the Brooks–Corey model). Water retention can only be predicted near saturation; this is due to the large error in estimating the air-entry parameter h_g .

CONCLUSIONS

The shape parameter of water retention curve n can be predicted from sand and clay content. This gives the Beerkan method more practical use in the field. In addition to the infiltration data, we now require only estimates of sand and clay content, and measurements of the initial and saturated moisture content using a low-cost frequency domain soil moisture probe (e.g., Gaskin and Miller, 1996). Many easy and inexpensive measurements can be performed to cover the large amount of spatial variation of soil hydraulic properties (Minasny and McBratney, 2002a).

It should be noted that the estimates refer to the “average” or “normal” soil. A spreadsheet containing a table of estimates of n , m , p_m , η , and c_p and their uncertainties as a function of sand and clay content (for the USDA and International systems) can be downloaded from our website (<http://tinyurl.com/syd8y>; verified 10 Apr. 2007). The website also contains Matlab codes for fitting the infiltration curve and predicting the soil hydraulic parameters.

ACKNOWLEDGMENTS

We wish to acknowledge the support of the Australian Research Council through its funding of a Linkage Project on Soil Inference Systems.

Table 4. Means and standard deviations of estimated water retention shape parameter n , hydraulic conductivity shape η , and water retention shape index p_m across USDA soil texture classes.

Texture	n		η		p_m	
	Mean	SD	Mean	SD	Mean	SD
Sand	2.77	0.296	5.59	0.923	0.60	0.189
Loamy sand	2.39	0.080	8.18	0.953	0.33	0.059
Sandy loam	2.27	0.039	10.49	1.081	0.24	0.032
Loam	2.20	0.028	12.76	1.351	0.19	0.024
Silt loam	2.22	0.047	12.18	2.182	0.20	0.039
Sandy clay loam	2.17	0.035	14.54	2.289	0.16	0.030
Clay loam	2.14	0.013	17.47	1.476	0.13	0.012
Silty clay loam	2.14	0.011	17.81	1.142	0.13	0.009
Silt	2.23	0.044	11.55	14.069	0.21	0.037
Sandy clay	2.11	0.021	20.90	4.222	0.11	0.019
Silty clay	2.12	0.009	19.77	1.192	0.11	0.008
Clay	2.10	0.015	22.66	3.637	0.10	0.013

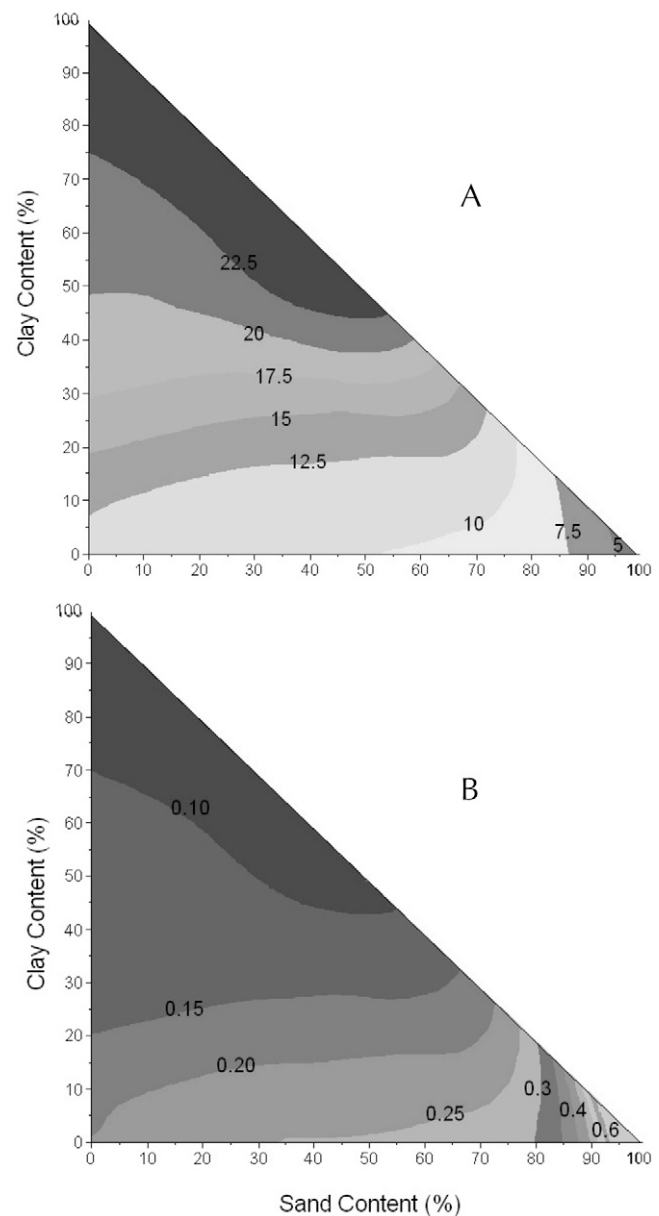


Fig. 5. Response surface of (a) predicted hydraulic conductivity shape parameter η and (b) predicted water retention shape index p_m as a function of sand and clay content.

Table 5. Means and standard deviations of the residuals of predicted hydraulic parameters, water retention (as water content θ at pressure heads 10–5000 mm), and hydraulic conductivity (K) using different methods for predicting n . Method 1 is the physically based method using porosity and the parameters of the particle size distribution (Eq. [5–9]); Method 2 prediction uses sand and clay content (Eq. [18]); Method 3 prediction uses texture class based on Table 3.

Parameter	Mean			SD		
	Method 1	Method 2	Method 3	Method 1	Method 2	Method 3
Water retention shape parameter n	0.11	−0.03	−0.04	0.27	0.27	0.24
Saturated hydraulic conductivity K_s , mm h ^{−1}	0.001	0.000	0.000	0.002	0.001	0.001
Scale parameter h_g , mm	−372.4	−392.8	−394.4	566.1	547.1	544.3
Hydraulic conductivity shape parameter η	−19.2	−21.2	−21.0	29.0	28.5	28.7
θ (10 mm), m ³ m ^{−3}	0.000	0.000	0.000	0.000	0.000	0.000
θ (100 mm), m ³ m ^{−3}	0.000	−0.001	−0.001	0.002	0.003	0.003
θ (1000 mm), m ³ m ^{−3}	−0.029	−0.015	−0.014	0.046	0.034	0.033
θ (5000 mm), m ³ m ^{−3}	−0.034	−0.018	−0.015	0.064	0.041	0.042
Log ₁₀ K (10), log ₁₀ (mm h ^{−1})	0.000	0.000	0.000	0.000	0.000	0.000
Log ₁₀ K (100), log ₁₀ (mm h ^{−1})	0.004	−0.005	0.000	0.010	0.015	0.003
Log ₁₀ K (1000), log ₁₀ (mm h ^{−1})	−0.094	0.294	−0.003	0.175	0.814	0.053

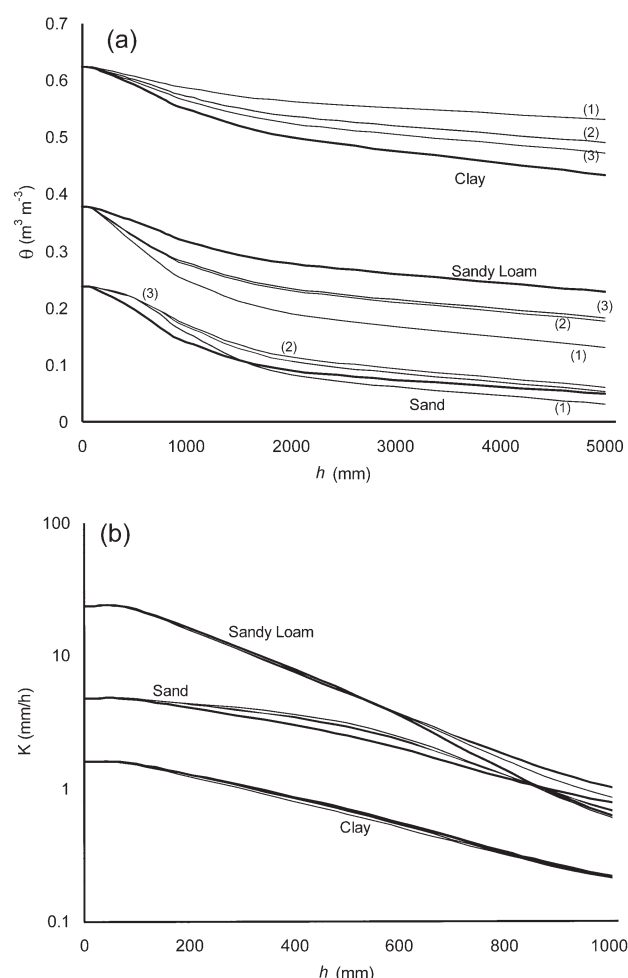


Fig. 6. Comparison of observed and predicted (a) water retention (water content θ vs. pressure head h) and (b) hydraulic conductivity (K) curves for sand, sandy loam, and clay. Observed values are represented as thick lines, while the others are lines with numbers next to the curves representing the method of prediction. The three methods for predicting n are: 1, from particle size distribution (PSD) and soil porosity η ; 2, from sand and clay content; and 3, soil texture class.

REFERENCES

Ancil, F., C. Michel, C. Perrin, and V. Andréassian. 2004. A soil moisture index as an auxiliary ANN input for stream flow forecasting. *J. Hydrol.* 286:155–167.

Braud, I., D. De Condappa, J.M. Soria, R. Haverkamp, R. Angulo-Jaramillo, S. Galle, and M. Vauclin. 2005. Use of scaled forms of the infiltration equation for the estimation of unsaturated soil hydraulics properties (the Beerkan method). *Eur. J. Soil Sci.* 56:361–374.

Breiman, L. 1996. Out-of-bag estimation. Tech. Rep. Statistics Dep., Univ. of California, Berkeley.

Brooks, R.H., and C.T. Corey. 1964. Hydraulic properties of porous media. *Hydrol. Pap.* 3. Colorado State Univ., Fort Collins.

Burdine, N.T. 1953. Relative permeability calculation from pore size distribution data. *Trans. Am. Inst. Miner. Metall. Pet. Eng.* 198:71–77.

Efron, B., and R.J. Tibshirani. 1993. An introduction to the bootstrap. *Stat. Appl. Probability Monogr.* 57. Chapman & Hall, London.

Fuentes, C., M. Vauclin, J.-Y. Parlange, and R. Haverkamp. 1998. Soil water conductivity of a fractal soil. p. 333–340. *In* P. Bayev et al (ed.) *Fractals in soil science*. Lewis Publ., Boca Raton, FL.

Gaskin, G.J., and J.D. Miller. 1996. Measurement of soil water content using a simplified impedance measuring technique. *J. Agric. Res.* 63:153–160.

Hastie, T., R. Tibshirani, and J. Friedman. 2001. The elements of statistical learning: Data mining, inference and prediction. *Springer Ser. Stat.* Springer-Verlag, New York.

Haverkamp, R., F.J. Leij, C. Fuentes, A. Sciortino, and P.J. Ross. 2005. Soil water retention: I. Introduction of a shape index. *Soil Sci. Soc. Am. J.* 69:1881–1890.

Haverkamp, R., P.J. Ross, K.R.J. Smettem, and J.-Y. Parlange. 1994. Three-dimensional analysis of infiltration from the disc infiltrometer. 2. Physically based infiltration equation. *Water Resour. Res.* 30:2931–2935.

Haverkamp, R., C. Zammit, F. Boubkraoui, K. Rajkai, J.L. Arrúe, and N. Heckmann. 1997. GRIZZLY, Grenoble soil catalogue: Soil survey of field data and description of particle-size, soil water retention and hydraulic conductivity functions. *Laboratoire d'Etude des Transferts en Hydrologie et en Environnement*, Grenoble, France.

Lassabatère, L., R. Angulo-Jaramillo, J.M. Soria Ugalde, R. Cuenca, I. Braud, and R. Haverkamp. 2006. Beerkan estimation of soil transfer parameters through infiltration experiments—BEST. *Soil Sci. Soc. Am. J.* 70:521–532.

Leij, F.J., W.J. Alves, M.Th. van Genuchten, and J.R. Williams. 1996. Unsaturated soil hydraulic database, UNSODA 1.0 user's manual. Rep. EPA/600/R-96/095. USEPA, Ada, OK.

Leij, F.J., R. Haverkamp, C. Fuentes, F. Zatarain, and P.J. Ross. 2005. Soil water retention: II. Derivation and application of shape index. *Soil Sci. Soc. Am. J.* 69:1891–1901.

Minasny, B., and A.B. McBratney. 2000. Estimation of sorptivity from disc-permeameter measurements. *Geoderma* 95:305–324.

Minasny, B., and A.B. McBratney. 2001. The Australian soil texture boomerang: A comparison of the Australian and USDA/FAO soil particle-size classification systems. *Aust. J. Soil Res.* 39:1443–1451.

Minasny, B., and A.B. McBratney. 2002a. The efficiency of various approaches to obtaining estimates of soil hydraulic properties. *Geoderma* 107:55–70.

Minasny, B., and A.B. McBratney. 2002b. The *neuro-m* method for fitting neural network parametric pedotransfer functions. *Soil Sci. Soc. Am. J.* 66:352–361.

Persson, M., B. Sivakumar, R. Berndtsson, O.H. Jacobsen, and P. Schjønning. 2002. Predicting the dielectric constant–water content relationship using artificial neural networks. *Soil Sci. Soc. Am. J.* 66:1424–1429.

Schaap, M.G., F.L. Leij, and M.Th. van Genuchten. 1998. Neural network analysis for hierarchical prediction of soil hydraulic properties. *Soil Sci. Soc. Am. J.* 62:847–855.

van Genuchten, M.Th. 1980. A closed-form equation for predicting the hydraulic conductivity of unsaturated soils. *Soil Sci. Soc. Am. J.* 44:892–898.